This is a pre-print copy. The final paper is available from the publisher's website https://www.nature.com/articles/s41437-020-0324-x and (free) here https://rdcu.be/b4ygt. DOI: 10.1038/s41437-020-0324-x

Heredity

Infection dynamics, dispersal, and adaptation: Understanding the lack of recovery in a remnant frog population following a disease outbreak

Running title: Understanding the lack of recovery in frog population

Donald T. McKnight[1,2]*, Leah J. Carr[1], Deborah S. Bower[1,2], Lin Schwarzkopf[1], Ross A. Alford[1], Kyall R. Zenger[1]

[1]College of Science and Engineering, James Cook University, Townsville, Queensland, Australia

[2]School of Environmental and Rural Science, University of New England, New South Wales, Australia

*Corresponding author email: donald.mcknight@my.jcu.edu.au

Words: 6700

Abstract

Emerging infectious diseases can cause dramatic declines in wildlife populations. Sometimes these declines are followed by recovery, but many populations do not recover. Studying differential recovery patterns may yield important information for managing disease-afflicted populations and facilitating population recoveries. In the late1980s, a chytridiomycosis outbreak caused multiple frog species in Australia's Wet Tropics to decline. Populations of some species (e.g., *Litoria nannotis*) subsequently recovered, while others (e.g., *Litoria dayi*) did not. We examined the population genetics and current infection status of *L. dayi*, to test several hypotheses regarding the failure of its populations to recover: 1) a lack of individual dispersal abilities has prevented recolonization of previously occupied locations, 2) a loss of genetic variation has resulted in limited adaptive potential, and 3) *L. dayi* is currently adapting to chytridiomycosis. We found moderate to high levels of gene flow and diversity (*Fst* range: <0.01–0.15; minor allele frequency: 0.192–0.245), which were similar to previously published levels for recovered *L. nannotis* populations. This suggests that dispersal ability and genetic diversity do not limit the ability of *L dayi* to recolonize upland sites. Further, infection intensity and prevalence increased with elevation, suggesting that chytridiomycosis is still limiting the elevational range of *L. dayi.* Outlier tests comparing infected and uninfected individuals consistently identified 18 markers as putatively under selection, and several of those markers matched genes that were previously implicated in infection. This suggests that *L. dayi*

has genetic variation for genes that affect infection dynamics and may be undergoing adaptation.

Introduction

Recent decades have seen a dramatic increase in emerging infectious diseases in wildlife. These diseases are caused by a diverse range of pathogens (including bacteria, fungi, and viruses) and have afflicted many taxa, often causing devastating declines or even extinctions (Daszak et al. 2000; Smith et al. 2006; Scheele et al. 2019). Diseases often shift from being epizootic to being enzootic, and in some cases, populations may rebound following an initial outbreak (Woodworth et al. 2005; McKnight et al. 2017a; Scheele et al. 2017). These recoveries are not guaranteed, and in any one area, some species may recover while others continue to either decline or persist only in low numbers (McKnight et al. 2017a; Bell et al. 2020). These differential recovery patterns among populations or species may hold important clues for understanding how wildlife populations respond to diseases, and understanding differential population responses may enhance conservation efforts and prevent or limit declines in other populations and species.

Chytridiomycosis presents a useful model to study differential recoveries. This disease is caused primarily by the fungal pathogen *Batrachochytrium dendrobatidis* (*Bd*) and has caused declines and extinctions in hundreds of amphibian species around the world (Berger et al. 1998; Daszak et al. 1999; Lips et al. 2006; Scheele et al. 2019). The Wet Tropics of Queensland, Australia experienced a large *Bd* outbreak in the late 1980s and early 1990s, during which several species declined, including green-eyed treefrogs (*Litoria serrata* [previously *genimaculata*]), waterfall frogs (*Litoria*

nannotis), and Australian lace-lid frogs (*Litoria* [previously *Nyctimystes*] *dayi*; Ingram and McDonald, 1993; Richards et al. 1993; Laurance et al. 1996; McDonald and Alford 1999). Historically, all three species occurred along rainforest creeks at most elevations; however, during the *Bd* outbreak, populations above 300–400m elevation (hereafter referred to as "upland") either declined sharply (*L. serrata*) or disappeared (*L. nannotis* and *L. dayi*), while lowland populations (< 300–400m) remained stable (Richards et al. 1993; Laurance et al. 1996; McDonald and Alford 1999). Following this initial decline, upland *L. serrata* populations quickly recovered at most sites, while *L. nannotis* gradually recolonised many, but not all, upland sites (McKnight et al. 2017a; Bell et al. 2020). Both of these species now have breeding populations at the headwaters of many upland creeks, despite the fact that *Bd* is still present and continues to infect both species (Richards and Alford 2005; McKnight et al. 2017a). In contrast, *L. dayi* has not recolonised upland sites and continues to be restricted to low elevations (McKnight et al. 2017a; Bell et al. 2020).

In a previous study (McKnight et al. 2019), we examined the population genetics of *L. serrata* and *L. nannotis* and found that both species have high levels of gene flow among populations but recovered upland populations have reduced genetic diversity. We also found that large areas of high-quality lowland habitat appeared to be important refugia for maintaining diversity during the outbreak. However, the question of why *L. dayi* has not recolonized the upland sites has yet to be addressed. Therefore, in the current

study, we built on our previous results by studying the current infection status and population genetics of *L. dayi*. We then compared our results for *L. dayi* to our previously published results on other species.

Specifically, we tested three hypotheses regarding the lack of upland recolonization in *L. dayi*: 1) *Litoria dayi* is restricted by low dispersal ability, which has prevented them from recolonising upland sites (null hypothesis: *L. dayi* has moderate or high dispersal ability, similar to other species in the area that have recovered from the outbreak); 2) The chytridiomycosis outbreak resulted in a genetic bottleneck reducing the genetic diversity required for adapting to the disease (null hypothesis: *L. dayi* has moderate or high genetic diversity, similar to other species in the area that have recovered from the outbreak); and 3) *Litoria dayi* is currently in the process of adapting to *Bd* (null hypothesis: *L. dayi* does not show evidence of adaptation). These three hypotheses were tested by examining current infection patterns, connectivity, and genetic diversity among regions, populations, and individuals, as well as searching for signatures of selection across the genome. These results were then compared to the previously published genetic patterns we documented for *L. serrata* and *L. nannotis* populations.

Materials and Methods

Study sites and samples

Toe tips (hereafter referred to as tissue samples) were collected from *L. dayi* populations in three areas: Wooroonooran National Park, Tully Gorge

National Park (hereafter “Tully”), and Girramay Range/Kirrama Range National Parks (Figure 1). Girramay and Kirrama border each other and share contiguous forests and streams; therefore, they will be referred to as a single site: “Girramay-Kirrama.” At each park, frogs were sampled for DNA at both the highest (~300–400m) and lowest (~50–200m) elevations currently occupied by *L. dayi* (Table 1). At Wooroonooran, frogs were sampled at two points along Pugh Creek. At Tully, *L. dayi* was sampled at Python Creek and an unnamed creek (both creeks feed into the Tully River), and at Girramay-Kirrama, frogs were sampled from two creeks at the current highest elevation for *L. dayi* (these sites correspond to “DCl” and “MRl” in our previous study on *L. nannotis* and *L. serrata*; McKnight et al. 2019). Both creeks connect below those sampling sites, so a third site was sampled downstream, at the lowest elevation for *L. dayi* at Girramay-Kirrama. At all three parks, there was a direct water connection between the highest and lowest elevation sites.

In addition to the tissue samples, we also collected data on the current infection status of *L. dayi* and examined how elevation influenced infection. The expectation was that if *Bd* is preventing *L. dayi* from recolonizing upland sites (as opposed to a lack of dispersal ability or genetic diversity), then both infection prevalence and intensity should increase with increasing elevation. To test this, skin swabs were collected from all captured frogs at each tissue sampling site, and frogs were swabbed at additional sites between our tissue sampling sites (two each at Tully and Wooroonooran, and one at Girramay-Kirrama). These sites were selected to cover the entire current elevation range

of *L. dayi*, with roughly evenly spaced sampling points at each park. More details on sampling sites and sample sizes are provided in Figure 1 and Tables 1 and 2.

At each site, frogs were sampled at night by walking a transect starting at the highest point where *L. dayi* could be found at upland sites, and at the lowest point where *L. dayi* could be found at lowland sites. Every *L. dayi* encountered was sampled until a minimum representative number (n~30) had been reached, or no more *L. dayi* could be found. At Girramay-Kirrama, *L. dayi* were rare, resulting in long transects, particularly at the lowest elevation; whereas at Tully, they were abundant, resulting in short transects (Table 1). Female *L. dayi* spend most of their time in the forest, and they are seldom found along streams (Hodgkison and Hero 1999). As a result, all samples were collected from males, with the exception of one female at Girramay-Kirrama, one female at Tully (swab only), and one juvenile at Tully. All sampling took place in September 2017, and each site was sampled during a single night or, if necessary, on 2 consecutive nights. No recaptures occurred when sampling took two nights.

Each frog was captured in a clean plastic bag, handled using a new pair of nitrile gloves, and released at its collection site within minutes of being captured. Tissue samples were collected *via* toe tips (one from each rear foot). This procedure is minimally invasive and does not typically result in bleeding. The scissors were dipped in ethanol and flame sterilized between each frog. Tissues were stored in vials of 70% ethanol. Skin swabs were collected by

rubbing a sterile, rayon-tipped swab (Medical Wire, MW113), along the stomach, thighs of each rear leg, and each rear foot (five times each, 25 strokes total). All samples were kept at room temperature for up to 48 hours, after which they were placed on ice for transport. Tissue samples were stored at 4°C and *Bd* swabs were stored at -20°C.

Bd *extraction, qPCR, and analysis*

To assess the infection status of *L. dayi*, the DNeasy Blood and Tissue DNA extraction kit (Qiagen) was used for each skin swab following the standard protocol with two modifications: an overnight digestion and two 20 µl elutions. The extracted DNA was sent to Cesar Australia, a commercial company, to perform triplicate qPCR following the standard protocol outlined in Boyle et al. (2004). Frogs were only considered *Bd* positive if *Bd* (≥ 0.1 zoospore equivalent) was identified in all three of the qPCR triplicates. Eighteen samples amplified in only one or two of the triplicates. These 18 samples were considered "ambiguous" and were removed from all analyses. To control for contamination, we made six blanks (i.e., clean swabs that were placed in vials without swabbing frogs) and extracted them and ran qPCR alongside the actual samples. There was no amplification in any of the blanks. Ceasar Australia also tested a subset of 31 samples for PCR inhibition using the TaqMAN Exogenous Internal Positive Control (VIC labelled) kit and did not find inhibition in any of the samples.

A binomial generalized linear regression model in R (R Core Development Team 2017) was used to look for an association between *Bd* infection prevalence (i.e., proportion of individuals that were infected) and elevation. Infection status was the response variable and elevation, park, and their interaction were the explanatory variables. All individuals were included regardless of infection status or intensity (excluding the 18 ambiguous samples). To test for an association between infection intensity (i.e., zoospore load) and elevation, a linear model in R was used. Infection intensity ($\log_{10}$ of qPCR results) was the response variable and elevation, park, and their interaction were the explanatory variables. All *Bd* positive individuals were included in this model, regardless of zoospore load. The significance of the relationships was tested using the Anova function in the car package (Fox and Weisberg 2011) with a type 2 sum of squares. For the binomial model, overdispersion was checkedby dividing the residual deviance by the degrees of freedom (1.17), and for the linear model, a residual plot and QQ plot were used to assess model fit.

Genomic DNA extraction and sequencing

Genomic DNA was extracted from each sample using the cetyl trimethyl ammonium bromide (CTAB) procedure (with a chloroform precipitation; Doyle and Doyle 1987), and the quality and quantity of DNA was checked using gel electrophoresis and a Nanodrop DNA/RNA spectrophotometer analyser. Genome-wide single nucleotide polymorphisms

209 (SNPs) were generated by Diversity Arrays Technology (DArT PL), Canberra
210 Australia, using their proprietary DArTSeq™ genotyping by sequence
211 methodology (Sansaloni et al. 2011; Kilian et al. 2012). This same approach
212 was previously used to generate the high quality SNP data for *L. serrata* and
213 *L. nannotis* that we used for comparisons (McKnight et al. 2019) and is
214 explained in detail elsewhere (Lal et al. 2017; Lind et al. 2017; Kjeldsen et al.
215 2019).

216 Briefly, DArTSeq™ SNP genotyping used both frequent and rare
217 restriction enzymes *Pst*I and *Sph*I, to perform a joint digestion-ligation
218 reaction at 37°C for two hours with approximately 100-200ng of individual
219 gDNA. Custom proprietary barcoded adapters were used in the ligation
220 reaction to facilitate individual sample recognition and allow for primer
221 binding sites. Each sample was individually PCR amplified using custom
222 primers to selectively enrich target fragments for sequencing and was
223 visualised via gel electrophoresis. Samples that displayed incomplete or non-
224 uniform digestion and amplification patterns were removed from the library. A
225 minimum of 15% random technical replicates was included for downstream
226 quality and performance measurements. Batches of individuals were pooled
227 and sequenced (77 cycles) on a single flow-cell lane on an Illumina HiSeq
228 2500 according to manufacturer's recommendations.

229 Individual raw fastq sequence data were de-multiplexed and adapters
230 trimmed with any individual read containing base pair Q-scores <30 removed.
231 All sequence data were checked against DArTdb database sequences to

identify read contamination for removal (Sivasankaran et al. 1993). SNP calling was conducted using the *DArTsoft14* software within the KDCompute analyses pipeline developed by Diversity Arrays Technology (http://www.kddart.org/kdcompute.html) following Lind et al. (2017) and Kjeldsen et al. (2019). KDCompute first created clusters (or stacks) of identical reads at a dataset level with three nucleotide mismatches allowed. These sequence clusters were then compared and matched to one another to identify polymorphisms. Following SNP identification, individual locus performance metrics were generated, including call rate, homozygote and heterozygote proportions, polymorphic information content (PIC), allele average read depth and reproducibility (based on technical replicates).

Post genotyping filtering and quality control

DArTSeq sequencing and filtering pipelines delivered a total of 33,016 SNPs. To obtain the highest quality data, SNPs were further filtered by first removing duplicate SNPs within the same sequence reads (69 base pairs) and sequences with a high degree of similarity (assigned with a 95% probability; Lal et al. 2017). Next, the following criteria were applied: average number of reads (averaged between the two alleles) ≥ 7, minor allele frequency (MAF) ≥ 0.02, call rate = 1.0 (i.e., no missing data), and reproducibility ≥ 0.9. A very stringent call rate was used because of the possible presence of null alleles at some parks (McKnight et al. 2019).

To identify potential outlier loci under selection, BayeScan v.2.1, (false discovery rate [FDR] = 0.1; Foll and Gaggiotti 2008; Foll 2012), HacDivSel (Carvajal-Rodriguez 2017), and FstHet (Flanagan and Jones 2017) were used both on the entire dataset (with each collection site as a population) and on each park separately (at Girramay-Kirrama, both higher elevation sites [G1 and G2] were entered as a single population; HacDivSel was not used for the entire dataset because it requires datasets within only two populations). This produced four sets of tests (one for the entire dataset and one for each park). Any markers that were identified as outliers in at least two programs for any of the four sets of tests were removed, producing a neutral data set. This procedure was used simply for the purpose of making a neutral data set (neutral among populations), not for identifying markers that were under selection specifically for *Bd*.

Once a neutral data set had been constructed, PLINK (v1.9; Purcell et al. 2007) was used to test for linkage disequilibrium (LD; all individuals were included in the analysis). Any links with an $R^2 \geq 0.6$ were removed. To minimize the loss of data, this was done by iteratively removing the SNPs with the greatest number of significant links until no links ≥ 0.6 remained.

The GWASExactHW package in R (v1.01; Painter and Washington 2013) was used to identify markers that were out of Hardy-Weinberg equilibrium (HWE). This test was performed with all the sites within each park combined into a single population. Any markers that were significantly out of HWE ($P < 0.01$) at all populations were removed (P values were not

277 adjusted for multiple comparisons, resulting in the retention of a conservative
278 set of markers).
279 These filtering steps resulted in a final dataset of 8,304 high quality,
280 neutral SNPs. With the exception of the call rate threshold and the filtering
281 criteria for neutral markers (i.e., outlier tests), these were the same filtering
282 steps used in McKnight et al. (2019) for *L. serrata* and *L. nannotis*.
283
284 *Population structure and connectivity*
285 Several methods were used to examine population structure and
286 connectivity, thus testing the hypothesis that *L. dayi* has low physical dispersal
287 abilities that are preventing it from recolonising the uplands. First, the genetic
288 distances among populations were calculated as *Fst* values in Arlequin
289 (v3.5.2.2; Excoffier et al. 2005). Second, the divMigrate function in the R
290 package diveRsity (v1.9.90; Keenan et al. 2013) was used to examine
291 differential migration rates.
292 Population structure was visualized using both NetView R (v1.0;
293 Steinig et al. 2015) and a Discriminant Analysis of Principal Components
294 (DAPC) via the R package "adegenet" (v2.0.1; Jombart 2008; Figure 1).
295 Additionally, an analysis of molecular variance (AMOVA) in Arlequin was
296 used to examine how the variance was partitioned among parks and within
297 parks (parks were included as the groups, with sampling sites within parks
298 included as the populations).
299

Genetic diversity

Genetic diversity was examined both within each sampling site and within each park (all sampling sites combined). The following metrics were calculated: minor allele frequencies (MAF), percent of markers that were polymorphic within a given site or park (both with and without rarefying), expected and observed heterozygosities (Genetix v4.05.2; Belkhir 2004), and *Fis* (Genetix). Additionally, the effective population size (N_e) was calculated using the LD method in NeEstimator, using only alleles with a MAF > 0.05 (v2.01; Do et al. 2014).

Adaptation

To construct a data set to identify markers under selection for *Bd*, the data were carried through the previously described filtering steps (except for removing outliers, removing SNPs in LD, and removing SNPs out of HWE) following the same settings used before, with one exception. Only using individuals that were not missing any data resulted in a large loss of markers. Therefore, to maximize the chance of detecting selection, a less-stringent threshold of 70% (i.e., less than 30% missing data) was used. Then, to reduce the presence of null alleles, for each SNP a Fisher's exact test was used to compare the amount of missing data among the three parks, and any SNPs that were significantly different at a false discovery rate (FDR) of 0.05 were removed.

Outlier tests were conducted in BayeScan (FDR = 0.1) (Foll and Gaggiotti 2008; Foll 2012), HacDivSel (Carvajal-RodrõÂguez 2017), and FstHet (Flanagan and Jones 2017). In each test, uninfected individuals were compared with individuals that were infected with a load equivalent to the DNA of at least ten zoospores. This threshold was selected *a priori* and was used to reduce noise in the tests by removing individuals who may have simply carried a few zoospores acquired from the environment without actually being infected.

The fundamental concept behind each outlier detection program is that alleles under selection will differ in frequency between two (or more) groups more strongly than the background difference between the groups (i.e., those markers are "outliers"). In our case, the expectation was that if an allele was under selection due to a role in *Bd* infection dynamics, the difference in the allele frequencies between infected and uninfected individuals would exceed the expected difference based on the background level of differentiation between those groups. Each program applies a different strategy to identify outliers (e.g., BayeScan uses a Bayesian approach based on the multinomial-Dirichlet model, whereas FstHet and HacDivSel apply frequentist methods), generally resulting in different outcomes from each method. Some of these results can be spurious for a variety of reasons, such as a mismatch between the evolutionary mechanism that produced the observed differences and the expected mechanism based on a program's assumptions. Therefore, we implemented a conservative approach and only considered markers significant

345 outliers (i.e., putatively under selection) if they were identified as outliers in
346 all three tests. This provided a robust set of markers that had a high probability
347 of being under selection.
348 We could not perform tests on subsets of the data (e.g., for an
349 individual park or elevation) due to small sample sizes for subsets. Therefore,
350 to control for differences among parks and elevations, the genetic distance (1-
351 proportion of shared alleles) among individuals was calculated using only the
352 markers that were identified as outliers in all tests. Then the adonis2 function
353 in the R package vegan (Oksanen et al. 2017) was used to run a
354 PERMANOVA with elevation and park as the first terms in the model,
355 followed by *Bd*, which was included as a binary factor (infected [≥ 10
356 zoospore equivalents] or uninfected [0 zoospore equivalents]). All interactions
357 were included (5,000 iterations). This tested whether infected and uninfected
358 individuals were genetically distinct (based on the markers that were
359 putatively under selection) after accounting for the effects of elevation and
360 park. To verify the utility of the PERMANOVA for this application, the
361 probability that a random subset of markers would return a significant
362 difference between infected and uninfected individuals was assessed by
363 repeatedly (1,000 iterations) randomly selecting 18 markers (the number that
364 were significant in all three outlier tests) and re-running the PERMANOVA
365 using only those markers to calculate genetic distance.
366 Additionally, for markers that were identified as outliers in all three
367 tests, an NCBI BLAST (blastn) search was used to align them with the

following genomes: *Xenopus* (taxid: 8353), *Rana* (taxid: 8399), and *Nanorana* (taxid: 120497). For each sequence, the best two matches (based on lowest E-value) were retained for further examination. An identical BLAST search was also conducted for four markers that were identified as outliers in both BayeScan (the most conservative method) and FstHet, but not HacDivSel (no markers were identified as outliers in BayeScan and HacDivSel, but not FstHet). NCBI, UniProt, GeneCards, and Xenbase were used to determine the putative functions of the genes.

Results

Infection status

Both *Bd* infection intensity ($F_{1,208} = 8.05$, $P = 0.005$) and prevalence ($X^2_{1,320}$, $P < 0.001$) increased significantly with increased elevation (Figures 2 and 3). There were also significant differences among parks in both analyses ($F_{2,208} = 6.36$, $P < 0.001$; $X^2_{2,320}$, $P = 0.021$; respectively), but interactions were not significant ($F_{2,208} = 0.54$, $P = 0.586$; $X^2_{2,320}$, $P = 0.137$; respectively). Infection prevalences at the highest elevations within each park were high, with 66.7–89.7% of individuals infected with *Bd*.

Low dispersal hypothesis

There was no evidence of genetic subdivision within parks (all $Fst \leq 0.04$) and only moderate differences among parks (all $Fst \leq 0.15$; Figure 1). Similarly, both NetView (Figure 1B) and DAPC (Figure 1C) showed that each

park clustered separately from the others, but there was little evidence of sub-structure within parks (nearly all of the variation in the DAPC was explained by differences among parks; Figure 1C). Further, the AMOVA found that differences among parks accounted for 9.05% of the variation in the data, whereas differences among sampling sites within parks only explained 1.55% of the variation (differences among individuals within sites = 2.11%; variation within individuals = 87.3%). The divMigrate results suggested that geneflow was bi-directional along the streams (Figure 1A).

Loss of genetic diversity hypothesis

Diversity analyses did not suggest inbreeding or a large loss of diversity (Table 3; Figure 4). Girramay-Kirrama had slightly reduced diversity compared to the other parks, but expected and observed heterozygosities were similar at all sites, and *Fis* values did not deviate substantially from zero. Similarly, average MAFs per site ranged from 0.192–0.245 and the percentage of polymorphic markers within each site ranged from 79.0–97.8%. Nevertheless, N_e estimates were low at Girramay-Kirrama (7.9–40.3 per site) and Wooroonooran (38.0–63.3 per site).

Adaptation hypothesis

BayeScan identified 22 outlier loci, HacDivSel identified 422, and FstHet identified 492 (550 markers total). Eighteen markers were identified as outliers by all three programs, and four were identified by BayeScan and

FstHet, but not HacDivSel (no markers were identified as outliers in BayeScan and HacDivSel, but not FstHet). The PERMANOVA based on the 18 consensus markers found a significant effect of *Bd* (pseudo $P < 0.001$) after accounting for elevation (pseudo $P < 0.001$) and park (pseudo $P < 0.001$); however, elevation and park explained more of the variation (elevation $R^2 = 0.137$, park $R^2 = 0.222$, *Bd* $R^2 = 0.062$). The only significant interaction was between elevation and park (pseudo $P = 0.005$; Supplementary Information). For the 1,000 PERMANOVAs using the same model structure and individuals, but random subsets of 18 markers, only 4.2% showed a significant effect of *Bd* (pseudo $P < 0.05$), which is close to the expected type 1 error rate. The lowest pseudo P value from random subsets of markers was 0.0026, whereas our pseudo P value for the 18 consensus markers was 0.0002. This suggests that it is unlikely that our results arose by chance, and the 18 consensus markers likely constitute an actual genetic difference between infected and uninfected frogs. This difference can be visualized with ordination plots (Figure 5).

The BLAST search found matches for all 22 of the potential outliers we tested (18 consensus markers + four that were found in BayeScan and FstHet but not HacDivSel). We could not find standard gene ontology terms for many of these sequences, therefore we used the information available in NCBI, UniProt, GeneCards, and Xenbase to assign the sequences into categories of putative functions or systems (see Supplementary Information for details about the SNPs and BLAST results). SNP sequences with the

highest BLAST scores (based on e-values [0.003–4.9]) were grouped into the following categories based on biological functionality (five fit into two categories): cell surface functions (recognition, movement, transport across the membrane) = 6, DNA/RNA (transcription, maintenance, repair) = 3, skin = 3, tumour regulation and apoptosis = 3, organelle structure and cytoskeleton = 3, nervous system = 3, immune system = 1, nuclear transport = 1, meiosis = 1, unknown or matches to full sequences rather than genes = 3. The second best BLAST matches (based on e-values) were similar (20 matches; three fit into two categories): cell surface functions (recognition, movement, transport across the membrane) = 3, skin = 3, tumour regulation and apoptosis = 3, organelle structure and cytoskeleton = 3, DNA/RNA (transcription, maintenance, repair) = 2, immune system = 1, nervous system = 1, GTPase activation = 1, unknown or matches to full sequences rather than genes = 6. Several of these (e.g., genes related to skin function and cell cycle regulation) have obvious implications for *Bd* and are consistent with previous studies. Nevertheless, it should be noted that due to the short length of our sequences and the lack of genomes for closely related species, many of these matches were low quality (only 10 markers had a match with an e-value <1, the remaining matches had e-values of 1.4 or 4.9).

Discussion

Our results suggest that *L. dayi* has both high population connectivity (consistent with effective dispersal) and high levels of genetic diversity

(comparable to those of *L. nannotis* and *L. serrata*). The results allowed us to test the hypotheses we advanced in the introduction regarding possible effects of dispersal, bottlenecking, selection, and ongoing infection on the lack of recovery in *L. dayi*.

Low dispersal hypothesis

Our results are not consistent with the hypothesis that low dispersal abilities have prevented *L. dayi* from recolonising upland sites. Population connectivity provides a useful proxy for dispersal ability, and we observed high levels of connectivity within each park (based on *Fst* values), and both NetView and the DAPC showed little evidence of structuring. Additionally, divMigrate did not detect asymmetry in the gene flow patterns, suggesting that frogs were moving both upstream and downstream. Although a downstream bias in gene flow is common in some stream-dwelling species (Bolnick et al. 2008; Guarnizo and Cannatella 2013), its absence in *L. dayi* makes sense, because their eggs are attached to rocks and their tadpoles possess adaptations to fast-flowing water, such as suctorial mouth discs and specialized tails, to prevent them from being washed downstream (Davies and Richards 1990).

The *Fst* values for *L. dayi* were similar to the previously reported values for *L. nannotis* (which went through the same pattern of declines but has recolonised many upland sites). Indeed, at Girramay-Kirrama, where our G1 and G2 sites correspond to *L. nannotis* sampling sites in McKnight et al. (2019), *L. dayi* only had a slightly higher *Fst* than *L. nannotis* (0.04 compared

to 0.01), and when looking across similar sites from each study, the ranges of *Fst* values were similar for both species (*L. dayi*: <0.01–0.04; *L. nannotis*: 0.01–0.08; only sites with direct water connections were included in these ranges). These results are also consistent with previous work showing that *L. dayi* move away from streams, with females spending most of the year in the forest (Hodgkison and Hero 1999).

Taken together, these results do not suggest a low dispersal ability in *L. dayi*. Indeed, the similarities to previously reported values and patterns for *L. nannotis* suggest that both species have similar dispersal abilities. Therefore, given that *L. nannotis* experienced the same declines, at the same sites, as *L. dayi*, but has recolonised many upland sites, a lack of dispersal ability in *L. dayi* does not appear to explain its lack of recovery. Another possibility, suggested by Bell et al. (2020), is that *L. dayi* has failed to recolonize upland sites because of limited dispersal opportunities due to small lowland population sizes, rather than an inherent lack of dispersal ability. Although this may have played a role at Girramay-Kirrama, *L. dayi* was abundant in the lowlands at Tully and Wooroonooran, making this hypothesis unlikely at those sites.

Additionally, the infection data showed that both the prevalence (percent of individuals infected) and intensity (zoospore load) of infections increased with elevation, with 66.7% or more of individuals infected at the highest elevations currently occupied by *L. dayi.* This result agrees with an *L. dayi* survey conducted in 2013 (Bell et al. 2020) and suggests that *Bd* is likely

still a substantial problem for *L. dayi* and continues to restrict its upper elevational range.

Loss of genetic diversity hypothesis

Litoria dayi had high levels of genetic diversity, and our results do not suggest that a lack of diversity has prevented them from adapting and recovering from the disease outbreak. Although the diversity was slightly lower at Girramay-Kirrama than at Wooroonooran or Tully, possibly as a result of *Bd* (McKnight et al. 2019), none of the parks showed obvious signs of inbreeding or low diversity. Several factors affect a population's ability to retain diversity during an outbreak, including the duration of the decline, the number of individuals that survived the decline, and gene flow from neighbouring populations (McKnight et al. 2017b). Thus, although diseases can cause a large loss of genetic diversity (Trudeau et al. 2004; Schoville et al. 2011; Albert et al. 2014; Serieys et al. 2015), many populations can endure a large population size reduction without experiencing bottlenecks or inbreeding (Morgan et al. 2008; le Gouar et al. 2009; Teacher et al. 2009; Lachish et al. 2011; Brüniche-Olsen et al. 2013). Populations of *L. dayi* at Wooroonooran and Tully appear to be robust, with high densities of individuals occurring over large areas (McKnight, pers. obs.). The species was less dense at Girramay-Kirrama, but still occurred over a large area. Additionally, based on the high levels of connectivity we observed, it is likely that our study populations benefitted from gene flow from populations we did not sample.

529 The large number of individuals surviving in the lowlands, combined with
530 geneflow, would allow the retention of high levels of genetic diversity, despite
531 the loss of all populations at sites above 300–400m elevation (Lachish et al.
532 2011; Whiteley et al. 2015; McKnight et al. 2017a; McKnight et al. 2019).
533 The observed diversity values for *L. dayi* were similar to previously
534 reported values for *L. serrata* and *L. nannotis* (McKnight et al. 2019). At
535 Girramay-Kirrama, *L. dayi* had slightly lower genetic diversity values than *L.*
536 *nannotis* and *L. serrata*, but comparing the species across all sites, *L. dayi* at
537 Wooroonooran and Tully generally had slightly higher genetic diversity than
538 did *L. serrata* or *L. nannotis* at Girramay-Kirrama (Figure 4). Further, at all
539 three parks, *L. dayi* generally had higher diversity than did either *L. serrata* or
540 *L. nannotis* at Paluma Range National Park. These comparisons are admittedly
541 strained due to the fact that, in some cases, different parks were sampled for
542 different species. However, the fact that *L. dayi* showed no signs of
543 inbreeding, and has not been able to recover even at parks with high diversity,
544 while *L. serrata* and *L. nannotis* both recovered even at sites with low
545 diversity, suggests that a lack of genetic diversity is not precluding *L. dayi*
546 from adapting to coexist with *Bd* at upland sites.
547 Effective population sizes for *L. dayi* (7.9–7499.3; median = 40.3)
548 were largely comparable to previously reported values for *L. nannotis* (18.4–
549 1756.5; median = 62.9) and *L. serrata* (10.3–676.1; median = 212.9)
550 (McKnight et al. 2019). Effective population sizes for *L. dayi* at
551 Wooroonooran and Girramay-Kirrama were generally low, but effective

552 population sizes were higher at Tully, particularly at site T2, which had the
553 highest density of *L. dayi* (based on the transect distance required to sample 30
554 frogs: 150m as opposed to 350–1,540m; median = 560m); this site was also
555 close to numerous other small creeks populated by *L. dayi*. The other sampling
556 sites were comparatively more isolated. We also note that Tully generally had
557 lower infection intensities and prevalences compared to the other sites.
558 Additionally, the low effective population size values at some sites may be
559 partially a sampling artefact, because female *L. dayi* live in the forest where
560 we could not sample them (Hodgkison and Hero 1999).
561
562 *Adaptation hypothesis*
563 Our results are consistent with the hypothesis that *L. dayi* is currently
564 undergoing adaptation to *Bd*. Previous research in other systems has
565 documented that there is a heritable component to *Bd* infection risk (Palomar
566 et al. 2016), and several studies have found evidence of *Bd* driving selection
567 (Grogan et al. 2018; Voyles et al. 2018; Kosch et al. 2019). Our results are
568 consistent with those studies. All three outlier tests identified the same 18
569 markers, and the subsequent PERMANOVA based on those markers
570 confirmed that infected and uninfected frogs were genetically distinct, even
571 after accounting for elevation and park. This suggests that selection for
572 resistance to *Bd* infection is occurring at those loci.
573 Additionally, the BLAST search matched several of the markers to
574 genes with potential implications for *Bd* infections. For example, five markers

matched genes related to skin function as either their best (3) or second-best (3) match (one matched for both). One of these (NCBI: XM_018268914.1; e-value = 1.4) was a keratin-associated protein, which is potentially of interest because *Bd* colonizes keratinized surfaces, resulting in electrolyte imbalances that can lead to death (Berger et al. 1998; Campbell et al. 2012). Further, three of the matches (e-values = 0.4–1.4) were for a fucosidase alpha-L gene (FUCA1; NCBI: XM_018564520.1), which was also implicated in *Bd* infection dynamics in southern corroboree frogs (*Pseudophryne corroboree*; Kosch et al. 2019). That study used a laboratory infection trial followed by genotyping each frog, and it used both outlier detection methods and a genome-wide association analysis to look for genes that were associated with *Bd* tolerance. Of 29 SNPs that they identified as potentially related to *Bd*, 20 matched fucosidase alpha-L genes. This agreement among studies is interesting, given that *L. dayi* and *P. corroboree* are not closely related. Nevertheless, there is good reason to suspect that fucosidase alpha-L genes would be involved in infection dynamics, because fucose is common on amphibian skin and likely plays a role in defence against pathogens, possibly by preventing them from binding to the skin (Meyer et al. 2007). Additionally, in mammals, fucosidase plays a role in the formation of the *stratum corneum*, the layer predominantly infected by *Bd* (Nemanic et al. 1983; Berger et al. 1998; Abdayem et al. 2016).

Several other genes are also noteworthy. For example, two of our sequences matched genes related to immune function (NCBI: KY587143.1

598 and XM_018243675.1; e-value = 4.9 and 1.4 respectively), one of which
599 (NCBI: KY587143.1) is associated with the MHC II complex. Additionally,
600 both our results and the results of Kosch et al. (2019) found an association
601 between *Bd* and the same sodium bicarbonate solute carrier, family 4 (slc4a9;
602 NCBI: XM_012959752.2; e-value = 4.9). Finally, four of our SNPs matched
603 genes involved in the regulation of tumours or apoptosis (two SNPs matched
604 for both the best and second-best match; e-value = 0.4–4.9). Two of those
605 genes were specifically related to tumour regulation in skin cells (NCBI:
606 XM_018560900.1 and XM_018560908.1). Genes that regulate cell
607 proliferation and apoptosis may have an important role in the progression of
608 *Bd* infections (Richmond et al. 2009). Indeed, a study that compared gene
609 expression in *Bd*-sensitive and tolerant species as well as between infected and
610 uninfected individuals found significant differences in a large number of genes
611 related to apoptosis (Ellison et al. 2014). Another study (Brannelly et al. 2017)
612 examined apoptosis in two species of experimentally infected frogs (including
613 a *Litoria* species) and found that infection load correlated positively with cell
614 death, further supporting the notion that apoptosis has an important role in
615 infections.
616 The agreement among outlier detection methods, agreement with
617 previous research, and biological plausibility of the genes identified, all
618 support the hypothesis that *L. dayi* is currently adapting to *Bd* or, at the least,
619 has genetic variation for traits that have important roles in *Bd* infections.
620 Nevertheless, several caveats should be acknowledged. First, the results of our

BLAST searches were often low-quality matches, reducing confidence in them. Second, this study was entirely observational. Therefore, although our results are suggestive, more work on *L. dayi* is needed before we can confirm that they are adapting to *Bd*. It would be particularly useful to employ techniques such as controlled heritability genetic parameter investigations and transcriptomics. Additionally, these efforts are currently hindered by a shortage of genetic resources for frogs in the family Pelodryadidae (and "treefrogs" more generally), and a reference genome for a member of this group would greatly enhance our ability to test for adaptation to *Bd*.

Mechanisms allowing recolonization

Our results suggest that *L. dayi* may be in the process of adapting to *Bd* despite a lack of upland recolonization. Therefore, it is worth briefly discussing how *L. dayi* could be adapting without experiencing upland population recoveries, as well as discussing other mechanisms that could allow recolonization. Although lowland populations of *L. dayi* have not experienced the massive declines that occurred in the uplands, our results show that many lowland individuals do become infected by *Bd*, particularly at the highest elevation sites (~300-400m) where they currently occur. These infections likely have fitness costs, even when they are sublethal (Chatfield et al. 2013; Campbell et al. 2019), which would result in selective pressure. The strength of that selective pressure is not clear, however, and it could take many generations before alleles that confer resistance or tolerance to *Bd* are common

644 enough in populations to allow the recolonization of upland sites (Robinson et
645 al. 2012). Here again, more research should be conducted on this species to
646 determine the strength of selection and follow populations for several
647 generations to attempt to document selection in action.
648 There are also several other potential explanations for the differential
649 recovery patterns of Australia's rainforest frogs that were beyond the scope of
650 this paper. For example, in some other systems, a shift in the timing of
651 reproduction has allowed populations to recover from declines associated with
652 *Bd* (Scheele et al. 2015). This has not been tested for our system, but it is
653 possible that *L. nannotis* and *L. serrata* underwent such a shift, while *L. dayi*
654 did not. Additionally, differences in skin microbial communities or anti-
655 microbial peptides may have played a role in the differential recovery patterns,
656 as has been suggested in other systems (Kueneman et al. 2016; Jani et al.
657 2017; Bates et al. 2018; Bell et al. 2018). We are investigating this possibility,
658 and our current results suggest that the skin microbiomes of *L. dayi* do differ
659 from those of *L. nannotis* and *L. serrata* (McKnight 2019 [unpublished
660 thesis]).
661 These possibilities are not mutually exclusive with the hypothesis that
662 adaptation to *Bd* is occurring. For example, fucose levels on the skin could
663 affect the microbiome, which could, in turn, affect *Bd.* Thus, adaptation may
664 be being driven by interactions between the microbiota and *Bd.* Such pathways
665 are clearly speculative, however, and future studies should continue to
666 examine this system, test these possibilities, and further our understanding of

667 the factors that allow some populations to recover while precluding recovery
668 in others.
669
670 *Conclusion*
671 We tested three hypotheses for the lack of upland recolonization in *L.*
672 *dayi*, and our results suggest that neither low dispersal abilities nor a lack of
673 genetic diversity can explain the absence of population recoveries. We did,
674 however, find consistent evidence that some loci are undergoing selection.
675 Thus, it is possible that *L. dayi* is currently in the process of adapting to resist
676 infection by *Bd*, but more research is needed to confirm this, ideally including
677 controlled heritability trials.
678
679 **Acknowledgements**
680 We are indebted to Eric Nordberg and Donna Simmons for their
681 assistance collecting these samples. Additionally, we would like to thank the
682 members of the Molecular Ecology and Evolution lab for their advice and
683 assistance with laboratory work. Finally, we would like to thank the Wet
684 Tropics Management Authority and James Cook University College of
685 Science and Engineering for funding this research. This work was conducted
686 under Department of Environment and Heritage Protection permits
687 #WITK16243115 and #WITK18531217, and with the approval of James Cook
688 University's animal ethics committee (#A2209 and #A2437).
689

Competing Interests

All authors affirm that they have no competing interests to declare.

Data Archiving

All data in this paper are available in the Supplementary Information. An identical copy is also available on Dryad (https://doi.org/10.5061/dryad.0gb5mkkz6).

Supplementary Information

Supplementary Information.xlsx = SNP data (raw, neutral, and used for outlier tests), *Bd* infection data, BLAST results, and metadata.

Literature Cited

Abdayem R, Formanek F, Minondo AM, Potter A, Haftek M (2016). Cell surface glycans in the human *stratum corneum*: distribution and depth-related changes. Exp Dermatol 25: 865–871.

Albert EM, Fernández-Beaskoetxea S, Godoy JA, Tobler U, Schmidt BR, Bosch J (2014). Genetic management of an amphibian population after a chytridiomycosis outbreak. Conserv Genet 16: 103–111.

Bates KA, Clare FC, O'Hanlon S, Bosch J, Brookes L, Hopkins K, et al. (2018). Amphibian chytridiomycosis outbreak dynamics are linked with host skin bacterial community structure. Nat Commun 9: 1–11.

Belkhir K (2004). Genetix 4.05.2. Univ Montpellier II, Lab Génome Popul

Montpellier, Fr.

Bell SC, Garland S, Alford RA (2018). Increased numbers of culturable inhibitory bacterial taxa may mitigate the effects of *Batrachochytrium dendrobatidis* in Australian Wet Tropics frogs. Front Microbiol 9: 1–14.

Bell, SC, Heard GW, Berger L, Skerratt LF (2020). Connectivity over a disease risk gradient enables recovery of rainforest frogs. Ecological Applications.

Berger L, Speare R, Daszak P, Green DE, Cunningham AA, Goggin CL, et al. (1998). Chytridiomycosis causes amphibian mortality associated with population declines in the rain forests of Australia and Central America. Proc Natl Acad Sci U S A 95: 9031–9036.

Bolnick D, Caldera E, Matthews B (2008). Evidence for asymmetric migration load in a pair of ecologically divergent stickleback populations. Biol J Linn … 94: 273–287.

Boyle DG, Boyle DB, Olsen V, Morgan JAT, Hyatt AD (2004). Rapid quantitative detection of chytridiomycosis (*Batrachochytrium dendrobatidis*) in amphibian samples using real-time Taqman PCR assayo Title. Dis Aquat Organ 60: 141–148.

Brannelly LA, Roberts AA, Skerratt LF, Berger L (2017). Epidermal cell death in frogs with chytridiomycosis (MÁ Esteban, Ed.). PeerJ 5: e2925.

Brüniche-Olsen A, Burridge CP, Austin JJ, Jones ME (2013). Disease induced changes in gene flow patterns among Tasmanian devil populations. Biol Conserv 165: 69–78.

736 Campbell CR, Voyles J, Cook DI, Dinudom A (2012). Frog skin epithelium:
737 electrolyte transport and chytridiomycosis. Int J Biochem Cell Biol 44:
738 431–434.
739 Campbell L, Bower DS, Clulow S, Stockwell M, Clulow J, Mahony M (2019).
740 Interaction between temperature and sublethal infection with the
741 amphibian chytrid fungus impacts a susceptible frog species. Sci Rep 9:
742 83.
743 Carvajal-Rodriguez A (2017). HacDivSel: Two new methods (haplotype-
744 based and outlier-based) for the detection of divergent selection in pairs
745 of populations. PLoS One 12: e0175944.
746 Chatfield MWH, Brannelly LA, Robak MJ, Freeborn L, Lilvaux SP, Richards-
747 Zawacki CL (2013). Fitness consequences of infection by
748 *Batrachochytrium dendrobatidis* in northern leopard frogs *Lithobates*
749 *pipens*. Ecohealth 10: 90–98.
750 Daszak P, Berger L, Cunningham AA, Hyatt AD, Green DE, Speare R (1999).
751 Emerging infectious diseases and amphibian population declines. Emerg
752 Infect Dis 5: 735–48.
753 Daszak P, Cunningham AA, Hyatt AD (2000). Emerging infectious diseases
754 of wildlife--threats to biodiversity and human health. Science 287: 443–
755 449.
756 Davies M, Richards SJ (1990). Developmental biology of the Australian hylid
757 frog *Nyctimystes dayi* (Gunther). Trans R Soc South Aust 114: 207–211.
758 Do C, Waples RS, Peel D, Macbeth GM, Tillett BJ, Ovenden JR (2014).

759 NeEstimator V2: re-implementation of software for the estimation of
760 contemporary effective population size (Ne) from genetic data. Mol Ecol
761 Resour 14: 209–214.
762 Doyle JJ, Doyle JL (1987). A rapid procedure for DNA purification from
763 small quantities of fresh leaf tissue. Phytochem Bull 19: 11–15.
764 Ellison AR, Tunstall T, Direnzo G V., Hughey MC, Rebollar EA, Belden LK,
765 et al. (2014). More than skin deep: Functional genomic basis for
766 resistance to amphibian chytridiomycosis. Genome Biol Evol 7: 286–298.
767 Excoffier L, Laval G, Schneider S (2005). Arlequin (version 3.0): An
768 integrated software package for population genetics data analysis. Evol
769 Bioinform Online 1: 47–50.
770 Flanagan SP, Jones AG (2017). Constraints on the FST-heterozygosity outlier
771 approach. J Hered 108: 561–573.
772 Foll M (2012). BayeScan v2.1 User Manual. Ecology 20: 1450–1462.
773 Foll M, Gaggiotti O (2008). A genome-scan method to identify selected loci
774 appropriate for both dominant and codominant markers: A bayesian
775 perspective. Genetics 180: 977–993.
776 Fox J, Weisberg S (2011). An R Companion to Applied Regression, 2nd edn.
777 Sage: CA.
778 le Gouar PJ, Vallet D, David L, Bermejo M, Gatti S, Levréro F, et al. (2009).
779 How Ebola impacts genetics of western lowland gorilla populations.
780 PLoS One 4.
781 Grogan LF, Robert J, Berger L, Skerratt LF, Scheele BC, Castley JG, et al.

(2018). Review of the amphibian immune response to chytridiomycosis, and future directions. Front Immunol 9: 1–20.

Guarnizo CE, Cannatella DC (2013). Geographic determinants of gene flow in two sister species of tropical Andean frogs. J Hered 105: 216–225.

Hodgkison SC, Hero J-M (1999). Seasonal behaviour of *Litoria nannotis*, *Litoria rheocola* and *Nyctimystes dayi* in Tully Gorge, North Queensland, Australia. In: Frogs in the Community: Proceedings of the Brisbane Symposium, http://www.qldfrogs.asn.au/, pp 29–39.

Ingram GJ, McDonald KR (1993). An update on the decline of Queensland's frogs. In: Lunney D, Ayers D (eds) Herpetology in Australia: A Diverse Discipline, Zoological Society of New South Whales: Mosman, NSW, pp 297–303.

Jani AJ, Knapp RA, Briggs CJ (2017). Epidemic and endemic pathogen dynamics correspond to distinct host population microbiomes at a landscape scale. Proc R Soc B Biol Sci 284: 20170944.

Jombart T (2008). adegenet: a R package for the multivariate analysis of genetic markers. Bioinformatics 24: 1403–1405.

Keenan K, McGinnity P, Cross TF, Crozier WW, Prodohl PA (2013). diveRsity: An R package for the estimation and exploration of population genetics parameters and their associated errors. Methods Ecol Evol 4: 782–788.

Kjeldsen SR, Raadsma HW, Leigh KA, Tobey JR, Phalen D, Krockenberger A, et al. (2019) Genomic comparisons reveal biogeographic and

anthropogenic impacts in the koala (*Phascolarctos cinereus*): a dietary-specialist species distributed across heterogeneous environments. Heredity 122: 525–544.

Kilian A, Wenzl P, Huttner E, Carling J, Xia L, Blois H, et al. (2012). Diversity Arrays Technology: A generic genome profiling technology on open platforms. Methods Mol Biol 888: 67–89.

Kosch TA, Silva CNS, Brannelly LA, Roberts AA, Lau Q, Marantelli G, et al. (2019). Genetic potential for disease resistance in critically endangered amphibians decimated by chytridiomycosis. Anim Conserv 22: 238–250.

Kueneman JG, Woodhams DC, Treuren W Van, Archer HM, Knight R, Mckenzie VJ (2016). Inhibitory bacteria reduce fungi on early life stages of endangered Colorado boreal toads (Anaxyrus boreas). ISME J 10: 934–944.

Lachish S, Miller KJ, Storfer A, Goldizen AW, Jones ME (2011). Evidence that disease-induced population decline changes genetic structure and alters dispersal patterns in the Tasmanian devil. Heredity 106: 172–182.

Lal MM, Southgate PC, Jerry DR, Bosserelle C, Zenger KR (2017). Swept away: ocean currents and seascape features influence genetic structure across the 18,000 Km Indo-Pacific distribution of a marine invertebrate, the black-lip pearl oyster *Pinctada margaritifera*. BMC Genomics 18: 66.

Laurance WF, McDonald KR, Speare R (1996). Epidemic disease and the catastrophic decline of Australian rain forest frogs. Conserv Biol 10: 406–413.

828 Lind CE, Kilian A, Benzie JAH (2017). Development of Diversity Arrays
829 Technology markers as a tool for rapid genomic assessment in Nile
830 tilapia, *Oreochromis niloticus*. Animal Genetics 48: 362–364.
831 Lips KR, Brem F, Brenes R, Reeve JD, Alford RA, Voyles J, et al. (2006).
832 Emerging infectious disease and the loss of biodiversity in a Neotropical
833 amphibian community. Proc Natl Acad Sci 103: 3165–3170.
834 McDonald KR, Alford RA (1999). A review of declining frogs in northern
835 Queensland. In: Campbell A (ed) Declines and Disappearances of
836 Australian Frogs, Envrionment Australia, pp 14–22.
837 McKnight D (2019). Life finds a way: The recovery of frog populations from
838 a chytridiomycosis outbreak. PhD Thesis. James Cook University.
839 McKnight DT, Alford RA, Hoskin CJ, Schwarzkopf L, Greenspan SE, Zenger
840 KR, et al. (2017a). Fighting an uphill battle: the recovery of frogs in
841 Australia's Wet Tropics. Ecology 98: 3221–3223.
842 McKnight DT, Schwarzkopf L, Alford RA, Bower DS, Zenger KR (2017b).
843 Effects of emerging infectious diseases on host population genetics: a
844 review. Conserv Genet 18: 1235–1245.
845 McKnight DT, Lal MM, Bower DS, Alford RA, Zenger KR (2019). The
846 return of the frogs: The importance of habitat refugia in maintaining
847 diversity during a disease outbreak. Mol Ecol 28: 2731–2745.
848 Meyer W, Seegers U, Schnapper A, Neuhaus H, Himstedt W, Toepfer-
849 Petersen E (2007). Possible antimicrobial defense by free sugars on the
850 epidermal surface of aquatic vertebrates . Aquat Biol 1: 167–175.

851 Morgan MJ, Hunter D, Pietsch R, Osborne W, Keogh JS (2008). Assessment
852 of genetic diversity in the critically endangered Australian corroboree
853 frogs, *Pseudophryne corroboree* and *Pseudophryne pengilleyi*, identifies
854 four evolutionarily significant units for conservation. Mol Ecol 17: 3448–
855 3463.
856 Nemanic MK, Whitehead JS, Elias PM (1983). Alterations in membrane
857 sugars during epidermal differentiation: visualization with lectins and
858 role of glycosidases. J Histochem Cytochem 31: 887–897.
859 Oksanen JF, Blanchet FG, Friendly M, Kindt R, Legendre P, McGlinn D, et al.
860 (2017). vegan: Community ecology package.
861 Painter I, Washington U of (2013). GWASExactHW: Exact Hardy-Weinburg
862 testing for Genome Wide Association Studies. R package version 1.01.
863 Palomar G, Bosch J, Cano JM (2016). Heritability of *Batrachochytrium*
864 *dendrobatidis* burden and its genetic correlation with development time
865 in a population of common toad (*Bufo spinosus*). Evolution 70: 2346–
866 2356.
867 Purcell S, Neale B, Todd-Brown K, Thomas L, Ferreira M, Bender D, et al.
868 (2007). PLINK: a toolset for whole-genome association and population-
869 based linkage analysis. Am J Hum Genet 81: 559–575.
870 Richards SJ, Alford RA (2005). Structure and dynamics of a rainforest frog
871 (*Litoria genimaculata*) population in northern Queensland. Aust J Zool
872 53: 229–236.
873 Richards SJ, McDonald KR, Alford RA (1993). Declines in populations of

874 Australia's endemic tropical rainforest frogs. Pacific Conserv Biol 1: 66–
875 77.
876 Richmond JQ, Savage AE, Zamudio KR, Rosenblum EB (2009). Toward
877 immunogenetic studies of amphibian chytridiomycosis: Linking innate
878 and acquired immunity. Bioscience 59: 311–320.
879 Robinson SJ, Samuel MD, Johnson CJ, Adams M, McKenzie DL (2012)
880 Emerging prion disease drives host selection in a wildlife population.
881 Ecol Appl 22: 1050–1059
882 Sansaloni C, Petroli C, Jaccoud D, Carling J, Detering F, Grattapaglia D, et al.
883 (2011). Diversity Arrays Technology (DArT) and next-generation
884 sequencing combined: genome-wide, high throughput, highly informative
885 genotyping for molecular breeding of Eucalyptus. BMC Proc 5: P54.
886 Scheele BC, Hunter DA, Skerratt LF, Brannelly LA, Driscoll DA (2015). Low
887 impact of chytridiomycosis on frog recruitment enables persistence in
888 refuges despite high adult mortality. Biol Conserv 182: 36–43.
889 Scheele BC, Pasmans F, Skerratt LF, Berger L, Martel A, Beukema W, et al.
890 (2019). Amphibian fungal panzootic causes catastrophic and ongoing loss
891 of biodiversity. Science 363: 1459 LP – 1463.
892 Scheele BC, Skerratt LF, Grogan LF, Hunter DA, Clemann N, Mcfadden M,
893 et al. (2017). After the epidemic: Ongoing declines, stabilizations and
894 recoveries in amphibians afflicted by chytridiomycosis. Biol Conserv
895 206: 37–46.
896 Schoville SD, Tustall TS, Vredenburg VT, Backlin AR, Gallegos E, Wood

897 DA, et al. (2011). Conservation genetics of evolutionary lineages of the
898 endangered mountain yellow-legged frog, *Rana muscosa* (Amphibia:
899 Ranidae), in southern California. *Biol Conserv* 144: 2031–2040.
900 Serieys LEK, Lea A, Pollinger JP, Riley SPD, Wayne RK (2015). Disease and
901 freeways drive genetic change in urban bobcat populations. Evol Appl
902 8: 75–92.
903 Sivasankaran RM, Purimetla B, Stankovic JA, Ramamritham K (1993).
904 Network services database-a distributed active real-time database
905 (dartdb) application, Proceedings of the IEEE Workshop on Real-Time
906 Applications 184–187
907 Smith KF, Sax DF, Lafferty KD (2006). Evidence for the role of infectious
908 disease in species extinction and endangerment. Conserv Biol 20: 1349–
909 57.
910 Steinig EJ, Neuditschko M, Khatkar MS, Raadsma HW, Zenger KR (2015).
911 NetView P: A network visualization tool to unravel complex population
912 structure using genome-wide SNPs. Mol Ecol Resour 16: 216–227.
913 Teacher AGF, Garner TWJ, Nichols RA (2009). Evidence for directional
914 selection at a novel major histocompatibility class I marker in wild
915 common frogs (*Rana temporaria*) exposed to a viral pathogen
916 (Ranavirus). *PLoS One* 4: e4616.
917 R Core Development Team (2017). R: A language and environment for
918 statistical computing.
919 Trudeau KM, Britten HB, Restani M (2004). Sylvatic plague reduces genetic

variability in black-tailed prairie dogs. J Wildl Dis 40: 205–211.

Voyles J, Woodhams DC, Saenz V, Byrne AQ, Perez R, Rios-sotelo G, et al. (2018). Shifts in disease dynamics in a tropical amphibian assemblage are not due to pathogen attenuation. Sceince 359: 1517–1519.

Whiteley AR, Fitzpatrick SW, Funk WC, Tallmon DA (2015). Genetic rescue to the rescue. Trends Ecol Evol 30: 42–49.

Woodworth BL, Atkinson CT, LaPointe DA, Hart PJ, Spiegel CS, Tweed EJ, et al. (2005). Host population persistence in the face of introduced vector-borne diseases: Hawaii amakihi and avian malaria. Proc Natl Acad Sci 102: 1531–1536.

Table 1. Study sites details. The coordinates represent the approximate midpoints of each transect. *Litoria dayi* were not abundant at Girramay-Kirrama, resulting in long transect distances, particularly at the lowest elevation, where they were clustered around small creeks that fed into the main channel. G1 and G2 correspond roughly to DCl and MRl (respectively) in McKnight et al. (2019).

Park	Site	Latitude	Longitude	Elevation mean (m)	Elevation range (m)	Transect length (m)
Girramay-Kirrama	G1	-18.17451	145.82828	303	283–327	610
Girramay-Kirrama	G2	-18.18250	145.80926	303	287–336	560
Girramay-Kirrama	G3	-18.16582	145.82360	222	214–225	310
Girramay-Kirrama	G4	-18.15697	145.82381	191	159–213	1540
Tully	T1	-17.77420	145.59390	378	359–423[a]	350[a]
Tully	T2	-17.76977	145.58993	275	258–286	220
Tully	T3	-17.76487	145.59011	198	195–207	330
Tully	T4	-17.77607	145.66484	95	91–100	150
Wooroonooran	W1	-17.38523	145.86868	319	295–356[b]	560[b]
Wooroonooran	W2	-17.38814	145.87605	237	224–247	250
Wooroonooran	W3	-17.39380	145.88595	134	126–143	200
Wooroonooran	W4	-17.39803	145.89468	57	47–64	450

[a]Only one frog was found above 398 m (210 m Transect length excluding that frog)
[b]Only one frog was found above 334 m (363 m Transect length excluding that frog)

Table 2. Sample sizes for each site. Tissue = tissue samples sequenced, All *Bd* swabs = all swabs that amplified in all three triplicates, *Bd* swabs for tissue samples = swabs that amplified in all three triplicates and were from frogs that were sequenced (one frog did not have a swab), *Bd*+ (≥ 10) = swabs that were *Bd* positive and had ≥ 10 zoospore equivalents of DNA, *Bd*+ (< 10) = swabs that were *Bd* positive but had < 10 zoospore equivalents of DNA, *Bd*- = swabs that showed no amplification in all three triplicates.

Site	Tissue	All *Bd* swabs				*Bd* swabs for tissue samples			
		Total	*Bd*+ (≥ 10)	*Bd*+ (< 10)	*Bd*-	Total	*Bd*+ (≥ 10)	*Bd*+ (< 10)	*Bd*-
G1	28	30	17	6	7	27	15	5	7
G2	19	18	8	8	2	18	8	8	2
G3	-	27	11	7	9	-	-	-	-
G4	23	28	11	8	9	21	9	5	7
T1	28	27	11	7	9	25	11	7	7
T2	-	27	9	12	6	-	-	-	-
T3	-	28	4	10	14	-	-	-	-
T4	28	29	4	6	19	26	2	5	19
W1	29	29	21	5	3	28	20	5	3
W2	-	29	18	5	6	-	-	-	-
W3	-	25	11	7	7	-	-	-	-
W4	28	29	2	6	21	28	2	5	21

Table 3. Diversity results for each site and for each park (i.e., all sites within a park combined). MAF = minor allele frequency, % poly. = percent of markers that were polymorphic at a given site, % poly. rare = percent of markers that were polymorphic at a given site after rarefying the data to the lowest sample size, H n.b. = expected heterozygosity (corrected), Het. obs. = observed heterozygosity, *Fis* (SD) = mean inbreeding coefficient and SD of the mean (median values ranged from -0.008–0.000), N_e = effective population size (via NeEstimator).

	Mean MAF (SD)	% poly.	% poly. rare	H n.b.	Het. obs.	*Fis* (SD)	N_e (jackknife CI) [NeEstimator]
G1	0.204 (0.158)	86.4	84.4	0.280	0.270	0.034 (0.200)	40.3 (22.2–114.7)
G2	0.192 (0.162)	79.0	79.0	0.265	0.272	-0.021 (0.246)	7.9 (4.8–12.5)
G4	0.204 (0.158)	85.1	84.0	0.281	0.282	-0.002 (0.218)	22.1 (9.9–98.5)
T1	0.243 (0.143)	97.5	96.3	0.333	0.323	0.033 (0.208)	67.7 (25.9–∞)
T4	0.243 (0.141)	97.8	96.3	0.334	0.321	0.044 (0.207)	7499.3 (3086.5–∞)
W1	0.236 (0.146)	95.6	94.1	0.324	0.315	0.028 (0.206)	63.3 (34.6–211.6)
W4	0.237 (0.146)	95.6	93.9	0.324	0.315	0.028 (0.210)	38.0 (19.1–150.2)
G	0.207 (0.157)	90.5	89.8	0.282	0.274	0.027 (0.143)	57.0 (40.7–86.1)
T	0.245 (0.140)	98.9	98.9	0.334	0.322	0.042 (0.157)	307.4 (124.8–∞)
W	0.241 (0.143)	97.6	97.6	0.327	0.315	0.039 (0.158)	87.3 (53.5–187)

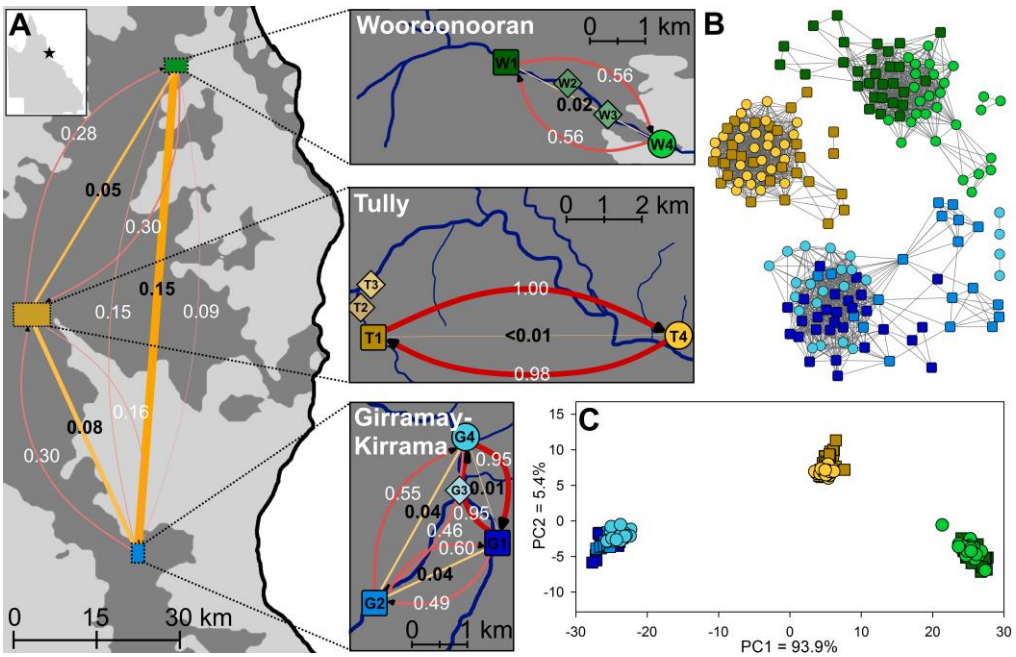

Figure 1. Study sites and connectivity. (A) Maps of study sites (symbols and colors correspond to panels 1B and 1C). Large squares = the highest elevation sites (sampled for genetics and *Bd*), large circles = the lowest elevation sites (sampled for genetics and *Bd*), small diamonds = mid-elevation sites (sampled for *Bd* only). Dark grey areas = rainforest, blue lines = streams, bold black numbers and orange lines = *Fst* values (the thickness and darkness of the lines are scaled with the *Fst*), white numbers and red lines = relative migration rates from divMigrate (arrows [black] indicate the direction of gene flow; all values are relative to each other with 1 being the highest level of migration observed; the darkness and thickness of the lines scale with the migration rates). (B) Results from NetView (k30) showing population structuring (all parks and populations were analysed together; lines = connections to up to 30 nearest neighbours; branch lengths are irrelevant and this should be read by looking at

975 the number and density of connections, rather than the exact placement of
976 points). (C) DAPC results visualizing structure among and within parks.
977
978

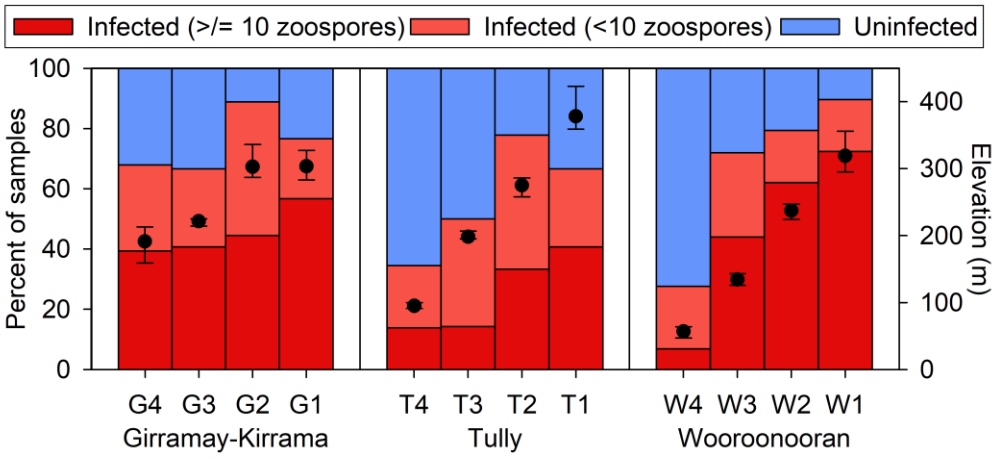

979

980 Figure 2. *Batrachochytrium dendrobatidis* infection prevalence at each study

981 site (i.e., percent of individuals that were infected). Sites within parks are

982 arranged from lowest elevation (G4, T4, W4) to highest elevation (G2, G1,

983 T1, W1). Black dots are the mean elevation for a given site, and the error bars

984 show the range.

985

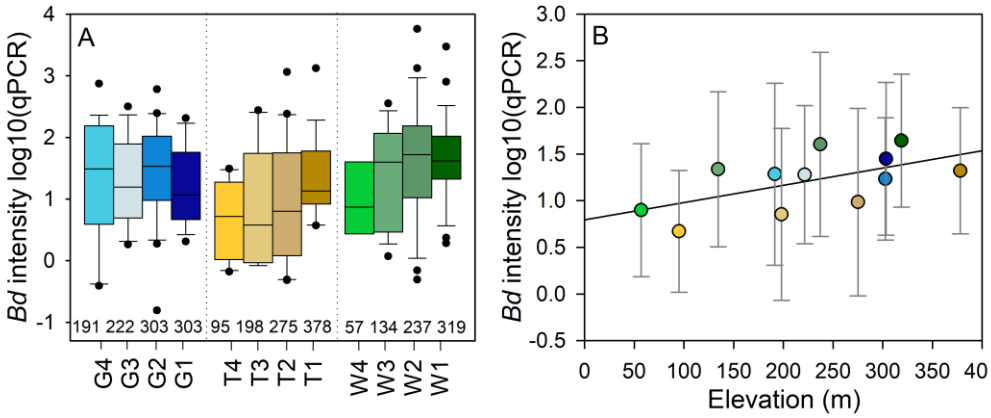

986

987 Figure 3. *Batrachochytrium dendrobatidis* infection intensity (i.e., $\log_{10}$ of the
988 zoospore load based on the qPCR results for all infected individuals). In both
989 panels, colors are used consistently and correspond to the sites in Figure 1. (A)
990 Infection intensity at each sampling site. Numbers show the mean elevation
991 per site. G = Girramay-Kirrama, T = Tully, W = Wooroonooran. Whiskers
992 show the 10^{th}/90^{th} percentile and all outliers are shown. (B) Mean infection
993 intensity for each site plotted against mean elevation for that site. Error bars
994 show one standard deviation for the infection intensity. Colors correspond to
995 sampling sites in Figure 1A.

996

997 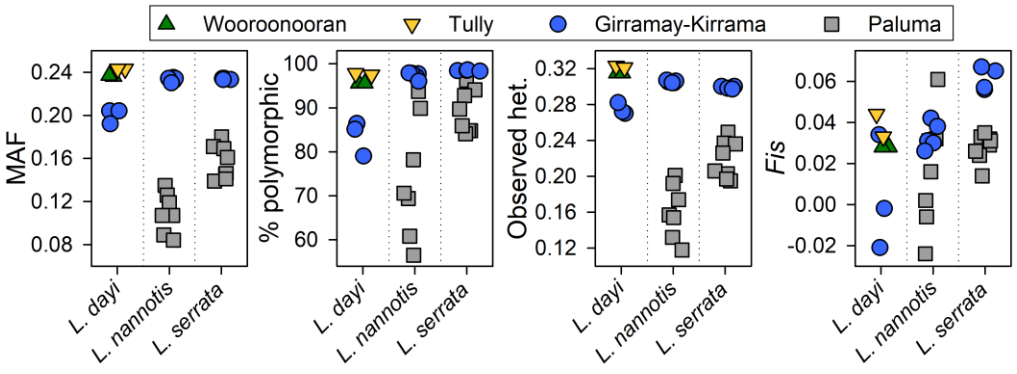

998 Figure 4. Genetic diversity metrics from this study (*L. dayi*) compared to the
999 previously reported results for *L. serrata* and *L. nannotis* (McKnight et al.
1000 2019). Each point is a sampling site. MAF = minor allele frequency, %
1001 polymorphic = percent of markers that were polymorphic in a given site,
1002 Observed het. = observed heterozygosity.

1003

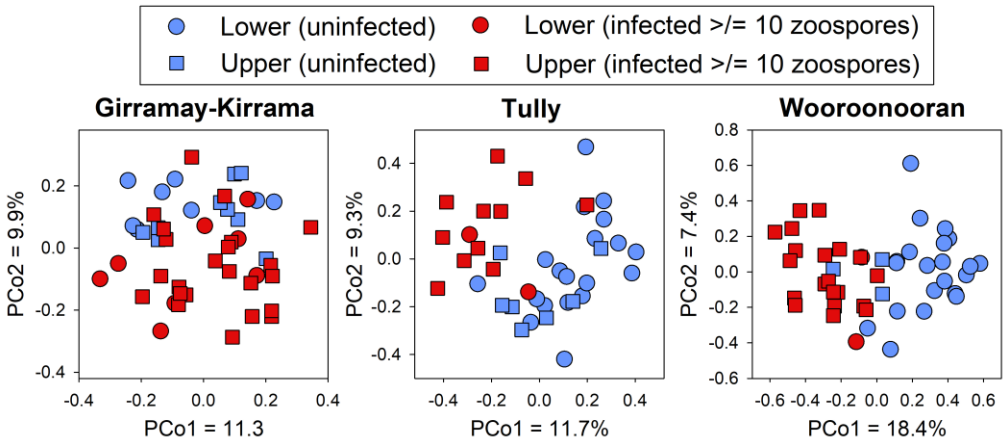

1004

1005 Figure 5. Ordination plots (PCoA) based on genetic distances (1-proportion of
1006 shared alleles) that were calculated using only the 18 SNPs that were
1007 identified as potentially being under selection in all three outlier detection
1008 tests. Lower = the lowest elevation site at each park (G4, T4, W4), Upper =
1009 the highest elevation site(s) at each park (G1, G2, T1, W1). Only individuals
1010 that were uninfected (0 zoospore equivalents) or infected with ≥ 10 zoospore
1011 equivalents were included.